Available online at www.sciencedirect.com
SCIENCE DIRECT®
ELSEVIER
Journal of the European Ceramic Society 25 (2005) 1717–1722
ECERS
www.elsevier.com/locate/jeurceramsoc

Subcritical crack growth processes in SiC/SiC ceramic matrix composites

R.H. Jones *, C.H. Henager Jr.

Pacific Northwest National Laboratory, MS P8-15, P.O. Box 999, Richland, WA 99352, USA

Available online 2 February 2005

Abstract

Ceramic matrix composites have the potential to operate at high temperatures and are, therefore being considered for a variety of advanced energy technologies such as combustor liners in land-based gas turbo/generators, heat exchangers and advanced fission and fusion reactors. Ceramic matrix composites exhibit a range of crack growth mechanisms driven by a range of environmental and nuclear conditions. The crack growth mechanisms include: (1) fiber relaxation by thermal (FR) and irradiation (FIR) processes, (2) fiber stress-rupture (SR), (3) interface removal (IR) by oxidation, and (4) oxidation embrittlement (OE) resulting from glass formation including effects of glass viscosity. Analysis of these crack growth processes has been accomplished with a combination experimental/modeling effort. Dynamic, high-temperature, in situ crack growth measurements have been made in variable $Ar + O_2$ environments while a Pacific Northwest National Laboratory (PNNL) developed model has been used to extrapolate this data and to add radiation effects. In addition to the modeling effort, a map showing these mechanisms as a function of environmental parameters was developed. This mechanism map is an effective tool for identifying operating regimes and predicting behavior. The process used to develop the crack growth mechanism map was to: (1) hypothesize and experimentally verify the operative mechanisms, (2) develop an analytical model for each mechanism, and (3) define the operating regime and boundary conditions for each mechanism. A map for SiC/SiC composites has been developed for chemical and nuclear environments as a function of temperature and time.

Keywords: Composites; Corrosion; Creep; Fracture; Carbides; Engine applications; Structural applications

1. Introduction

Silicon carbide is a refractory semiconductor with unique properties. Because of its thermal, mechanical and chemical stability, it can be used in extremely harsh environments. Pure SiC also provides exceptionally low radioactivity under neutron radiation, making it a top candidate for use in advanced fission and fusion reactors. However, these applications will require that these composites be optimized for maximum performance. To accomplish this it will be necessary to understand their high-temperature mechanical, chemical and radiation properties. Ceramic composites made from silicon carbide fibers and silicon carbide matrices (SiC_f/SiC) are promising because of their excellent high-temperature strength, fracture, creep, corrosion and thermal shock resistance. The continuous fiber architecture, coupled with engineered interfaces between the fiber and matrix, provide excellent fracture properties and fracture toughness values on the order of 25 MPa $m^{1/2}$. The strength and fracture toughness are independent of temperature up to the limit of the fiber stability. Also, these fiber/matrix microstructures impart excellent thermal shock and thermal fatigue resistance to these materials so start-up and shut-down cycles and coolant loss scenarios should not induce significant structural damage. For nuclear applications, the radiation resistance of the β phase of SiC imparts excellent radiation resistance. The β phase of SiC has been shown by numerous studies to have a saturation swelling value of about 0.1–0.2% at 800–1000 °C. This suggests that composites of SiC/SiC have the potential for excellent radiation stability. The purpose of this paper is to describe the subcritical crack growth behavior of SiC_f/SiC composites as this is an element in the creep behavior of these materials. This analysis is based on the development of crack growth models and the supporting experimental data.

* Corresponding author. Tel.: +1 509 376 4276; fax: +1 509 376 0418.
E-mail address: rh.jones@pnl.gov (R.H. Jones).

0955-2219/$ – see front matter © 2004 Elsevier Ltd. All rights reserved.
doi:10.1016/j.jeurceramsoc.2004.12.015

2. Subcritical crack growth in SiC/SiC

2.1. Mechanisms and model development

Pacific Northwest National Laboratory (PNNL) was among the first to identify and study time-dependent bridging in ceramic composites[1–3] and we have proposed a crack growth mechanism map based on available experimental data as a function of temperature and oxygen partial pressure for continuous fiber composites with carbon interphases[4]. An approach to modeling dynamic time-dependent crack bridging has emerged from the work of Bückner[5] and Rice[6] based on the use of weight-functions to calculate crack-opening displacements[7]. Once a relationship[8,9] between crack-opening displacement and bridging tractions from crack-bridging elements is included, a governing integral equation is obtained that relates the total crack opening, and the bridging tractions, to the applied load. The solution of this equation gives the force on the crack-bridges and the crack-opening displacement everywhere along the crack face[5–7,10]. Begley et al.[11] first developed a dynamic model and applied it to a variety of time-dependent bridging cases for linear creep laws[12–14]. Recently, a more appropriate bridging relation for creeping fibers has been developed by Cox et al.[9] that provides axial and radial stresses in creeping fibers with linear and non-linear creep laws.

We have developed a similar bridging law for non-linear creeping fibers that also considers the case for interface removal due to oxidation. We treat discrete fiber bridges as opposed to a bridging force distribution because each fiber has a different environmental exposure. A non-linear (in time and stress) creep law is used to compute bridge extensions.

2.2. Environmental effects: model and mechanism map

2.2.1. Compliance of a frictionally bonded fiber (bridge)

We introduce an expression for the compliance of a bridging fiber, Φ_b, using the assumptions of frictional bonding with a weak, debonding interphase. The frictionally bonded fiber involves an unbonded or free length, l_{free}, and a debonded or frictionally bonded and sliding length, l_{deb}, for a fiber bridging a crack of opening u_t, as shown in Fig. 1.

The free length of fiber, which is not subject to frictional forces, is assigned a compliance, Φ_b^l, and the portion of the fiber subjected to a frictional sliding resistance along length l_{deb} due to P_f (Fig. 1) is assigned a non-linear compliance, Φ_b^n, such that $\delta_b = \Phi_b^l P_b + \Phi_b^n P_b^2$ [15], where P_b is the 2D normalized bridge force and δ_b, is the bridge displacement. As suggested by Cox et al.[9] one could include a time-dependent debonding from fiber contraction due to Poisson effect and creep deformation, which provides an additional time-dependent fiber compliance term.

2.2.2. Fiber relaxation (FR) due to creep

The time-dependent extension of a fiber bridge at elevated temperatures obeys a power-law creep equation for Nicalon-CG and Hi-Nicalon fibers as:

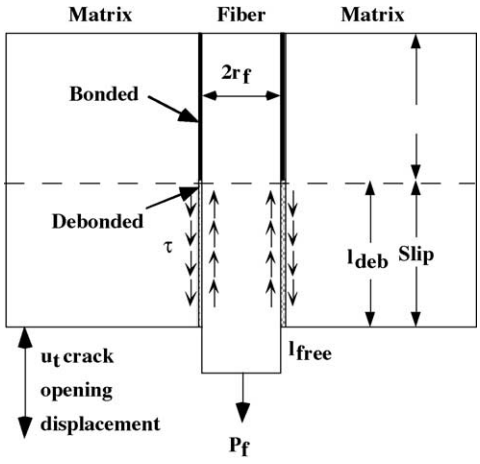

Fig. 1. Schematic of frictionally bonded fiber acted upon by force P_f due to debonding and sliding across a Mode I crack with opening u_t. The lengths l_{deb} and l_{free} are shown.

$$\varepsilon_f = A\sigma^n t^p \exp\left(\frac{-pQ}{RT}\right) = C(T)\sigma^n t^p \Rightarrow \dot{\varepsilon}_f = C(T)\sigma^n pt^{p-1} \quad (1)$$

where A is a constant, t is time, Q is an activation energy for creep, R is the gas constant and T is temperature, n is the stress exponent, p is the time–temperature exponent, σ is stress, E_f is the fiber strain and $C(T)$ is $A\exp(-pQ/RT)$. The unbonded length given by l_{free} creeps at the bridging stress applied to the fiber. The portion of fiber that is debonded creeps at a stress that varies over the debond length, which is found by integration. The creep extension of a bridge becomes:

$$\Delta l_{free} = C(T)pt^{p-1}\Delta t\left(\frac{P_b}{2r_f}\right)^n l_{free} \quad (2)$$

for the free length of fiber and

$$\Delta l_{deb} = C(T)pt^{p-1}\Delta t\int_0^{l_{deb}}\sigma^n(z)\mathrm{d}z = C(T)pt^{p-1}\Delta t \times\left(\frac{P_b}{2r_f}\right)^n l_{deb}\left(1-\frac{1}{(1+\xi)^n(1+n)}\right) \quad (3)$$

for the debonded length when the axial fiber stress is given by:

$$\sigma(z) = \frac{P_b}{2r_f} - \frac{2\tau z}{r_f} \quad (4)$$

where t is the total creep time, Δt is the time step, z is the axial distance along the fiber measured from the crack face, τ is the shear stress and ξ is given by $fE_f/(1-f)E_m$. Time, t, is referenced to the inception of each bridge into the bridging zone and is tracked separately for each bridge.

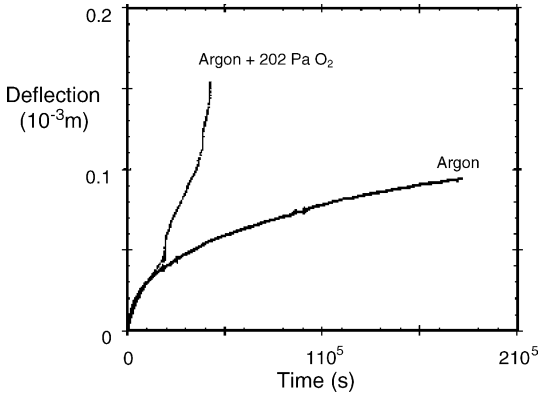

Fig. 2. Displacement-time curves for single-edge notched beam bars of SiC/SiC Hi-Nicalon composites tested at 1373 K in 4-point bending for the indicated time. In Ar the curve follows the expected fiber creep laws while in Ar + O_2 the curve becomes linear in time as given by Eq. (5).

2.2.3. Fiber/matrix interphase removal (IR) by oxidative volatilization

When the fiber/matrix interphase is a material that can undergo a gaseous reaction with oxygen then interphase removal in oxygen-containing environments becomes important, as shown by the data in Fig. 2. Previous research has shown that the following interphase recession data applies to the typical 0/90 plain weave CVI-SiC/SiC_f materials with a CVI carbon interphase[17].

$$l_{ox} = 3.3 \times 10^{-4} e^{-6014/T} P_{o_2}^{0.889} t = R_i(T, P_{o_2})t \quad \text{thus}$$
$$\Delta l_{ox} = R_i(T, P_{o_2})\Delta t \tag{5}$$

where l_{ox} is the recession distance along the fiber/matrix interphase from the crack face into the composite in m/s, T is temperature in K, P_{o_2} is fractional oxygen concentration, t is exposure time and R_i is the interface recession rate. We assume that l_{deb} is maintained at its value determined by τ and the load on the fiber.

2.2.4. Oxidation of the bridging fiber (OE and VS/OE)

Exposed bridging fibers will undergo oxidation at elevated temperatures according to:[18]

$$fib_{ox} = 1.84 \times 10^{-7} e^{-4016.8/T} P_{o_2} t^{0.5} \tag{6}$$

where fib_{ox} is the oxide thickness grown on the fiber in m, T is temperature in K, P_{o_2} is fractional oxygen concentration, and t is exposure time in s.

2.2.5. Fiber stress rupture (SR)

Exposed bridging fibers will obey time-dependent stress rupture relationships as:[19]

$$\ln(\sigma_f) = 2.3E - \left(\frac{\beta}{R}\right)[RT(\ln(t) + C)] \tag{7}$$

where σ_f is fiber strength in MPa, and E, β, and C are fitted parameters from single fiber rupture tests in air.

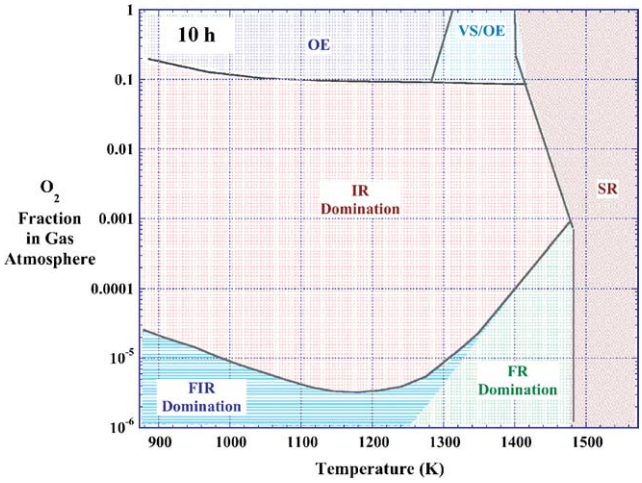

Fig. 3. Map showing regions of dominant crack growth mechanism as a function of oxygen concentration in the environment and temperature for SiC/SiC composites.

2.3. Crack growth mechanism map

The proposed mechanism map is shown in Fig. 3. Fiber creep relaxation (FR) dominates at high temperatures and low oxygen concentrations, as expected, since creep activation energies are high (~600 kJ/mol) and oxidation activation energies are low (~50 kJ/mol). Crack extension is dominated by interface removal (IR) for oxygen concentrations less than ~0.1 when the temperatures are not extreme. We observe both kinetic and activation energy changes in our experimental data consistent with this hypothesis. We define the transition from FR to IR by the locus of points where the crack growth from each mechanism is equal. At higher oxygen concentrations, the fiber/matrix interphase oxidizes and is replaced by a glass phase and either oxidation embrittlement (OE) or viscous sliding (VS) mechanisms may occur. We propose that interphase glass formation and channel pinch-off (fiber–matrix bonding) at intermediate temperatures where the resultant glass phase is brittle results in OE and the fibers fail since they can no longer slide relative to the matrix. We define the transition from IR to OE as the locus of points where the fiber/matrix channel pinches-off and OE occurs in a finite crack growth increment (2.5 mm in this case). At higher temperatures the glass phase is viscous, not brittle and VS occurs. When the glass phase has a high viscosity, fibers can fail by rupture since the local fiber/matrix bonding leads to stress concentrations[20], rather like replacing an interface with a low frictional sliding stress with a higher one. It follows that there will be a temperature above which this stress concentration will not fail the fibers but this will depend on the details of the compositionally dependent glass viscosity. The transition from OE to VS/OE is schematic since we do not yet know the glass viscosity nor have we implemented a viscous sliding treatment for the model, although such treatments exist[21]. Fiber oxidation also results in loss of strength, which leads to embrittlement via

fiber stress rupture[16,22,23]. Fiber stress corrosion should be accounted for by the SR mechanism since this data was obtained in air. Since predicted fiber stresses in the crack wake of a dynamic crack are on the order of 800 MPa or smaller, SR is difficult to achieve until temperatures above about 1400 K.

2.4. Irradiation induced creep crack growth (FIR)

2.4.1. Irradiation enhanced creep of SiC fibers

The earliest studies of irradiation-enhanced creep of SiC were reported by Price[24] who conducted bend stress relaxation of monolithic β-SiC strips. These strips were held at a fixed strain and irradiated at 780, 950 and 1130 °C with neutrons in the EBR II fast reactor to a dose of 7.7×10^{25} n/m^2. Price reported a substantial enhancement over thermal creep over this temperature range. More recent studies by Scholz et al.[25] have shown that a similar and even larger creep effect was found for β-SiC fibers (SCS-6) irradiated with light ions. Over the same temperature range as that reported by Price[24], the light ion irradiated SiC fibers exhibited a 100×'s faster creep rate. Relative to the thermal creep rate at 1000 °C, the irradiation creep rate for the neutron irradiated bulk SiC reported by Price[24] was 100×'s faster while the light ion irradiated fibers was 10,000 times faster. The FR domination regime in Fig. 3 results from thermal creep of the fibers. Clearly, the irradiation enhanced creep rate will also cause creep crack growth and must therefore be considered for nuclear applications.

2.4.2. Irradiation enhanced creep of SiC/SiC composites

There is no existing irradiation creep data for SiC/SiC composites as there is for fibers. Therefore, it is necessary to rely on model predictions of the effects of irradiation on creep crack growth. A dynamic crack growth model developed by Henager and Hoagland,[15] has been used to predict irradiation enhanced creep effects on crack growth. We observe that irradiation creep of the fibers dominates the fiber deformation process for temperatures below 1273 K (1000 °C) but thermal creep dominates at higher test temperatures, Fig. 4. This implies that we will need to further understand and model irradiation creep processes in SiC-based fibers since apparently that process is important in applications that operate at or below 1000 °C.

2.5. Fiber relaxation due to thermal and irradiation creep

The time-dependent extension of a fiber bridge at elevated temperatures still obeys the power-law creep as given by Eq. (1) but now also has a portion that is proportional to the irradiation dose rate and stress. Scholz[25] showed that irradiation creep could be given as:

$$\dot{\varepsilon} = K\dot{\phi}\sigma \tag{8}$$

where K is the irradiation creep compliance for a given material, $\dot{\phi}$ is the dose rate in dpa s^{-1}, and σ is the applied stress. For SiC a value of 4.7×10^{-6} MPa^{-1} dpa^{-1} is used for K. Then, in analogy with the thermal creep analysis but using a linear stress relationship gives:

$$\Delta l_{\text{free}} = K\dot{\phi}\frac{P_{\text{b}}}{2r_{\text{f}}}\Delta t l_{\text{free}} \tag{9}$$

for the free length of fiber and

$$\Delta l_{\text{deb}} = K\dot{\phi}\frac{P_{\text{b}}}{4r_{\text{f}}}\Delta t l_{\text{deb}} \tag{10}$$

for the debonded length of fiber. These terms are then added using superposition to the thermal creep terms to give the total elongation of the bridging fibers from simultaneous thermal and irradiation creep. The model can then be run to study the relative rates of each mechanism.

3. Discussion

The materials included in the map (Fig. 3) are 2D woven SiC/SiC composites with Nicalon-CG fibers at ∼40% by volume. Lewinsohn et al.[4] discuss the map concept, the materials, and the experimental data more fully. However, we have observed that temperature and oxygen concentration play the most important roles in determining the operable crack growth mechanisms. Therefore, it was imperative to include oxidation in the dynamic crack model in addition to the non-linear fiber creep. However, additional modeling remains and more experimentation is planned.

Crack growth appears to be controlled by FR above the composite matrix-cracking threshold at elevated temperatures in inert environments. PNNL and others have determined composite deformation rates[1,2,26–37] and activation

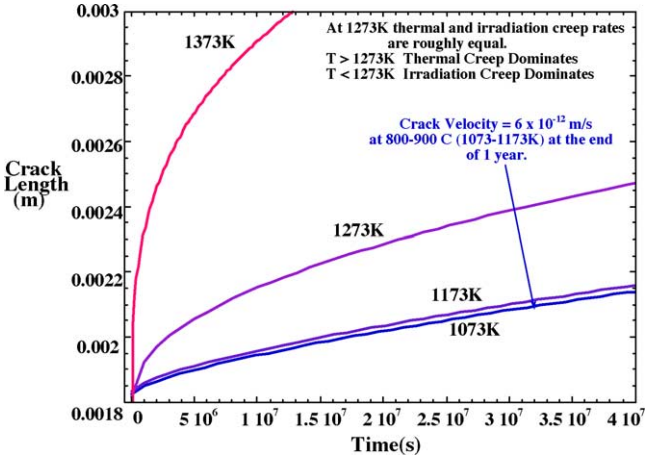

Fig. 4. Irradiation creep as a function of temperature of SiC/SiC composite with Hi-Nicalon fibers using a fission damage spectrum and damage rate of 0.44 dpa/year. The curves shown include thermal and irradiation creep of the bridging fibers. At 1273 K the thermal crack velocity is equal to the irradiation-induced crack velocity. Note that the crack velocities are not steady state velocities but continue to decrease with increasing time.

energies under these conditions and they match quite well with activation energies for fiber creep, about 500–600 kJ/mol. Our dynamic crack growth model agrees reasonably well with measured crack growth rates and these activation energies.

When oxygen is introduced during the crack growth testing the deformation rates increase and the activation energy decreases to about 50 kJ/mol, in agreement with carbon oxidation processes. Significantly, the crack growth kinetics change from non-linear to linear since now the bridge compliance is dominated by the linear portion as $l_{free} + l_{ox}$ approach and exceed l_{deb}, Fig. 2. Again, our model agrees well with these changes in both kinetics and activation energies. The transition between the FR and IR mechanisms is defined as the locus of points where the crack growth rates of each mechanism are roughly equal. This was determined by choosing an oxygen concentration where the crack velocity doubled compared to the velocity without any oxygen. This curve is steep as shown in Fig. 2 due in part to the high activation energy of the fiber creep process. It is bounded at high temperatures by fiber stress rupture mechanisms.

Transitions from IR to either OE or VS/OE mechanisms are shown. We find that there is a competition between specimen failure due to IR relative to the time for pinch-off and OE to occur. The dynamics are handled by removing those fibers from the bridging zone that have an oxide thickness greater than some critical value, such as the interphase thickness. However, this transition is crack length (specimen size) and interphase thickness dependent. The size effect occurs since OE depends on total fiber exposure time, which is dependent on crack length. Interphase thickness effects arise due to our criterion that pinch-off occurs prior to the onset of OE. The computations shown here are for an interphase thickness of 150 nm. Other plausible OE mechanisms only require a critical oxide thickness that is not interphase thickness dependent[38,39]. However, such mechanisms will still exhibit a specimen size effect or history effect. Transitions from OE (pinch-off with brittle glass phase) to VS/OE (non-brittle, viscous glass phase) depend on the viscosity of the glass which is strongly dependent on glass composition. Thus, these transitions are not rigorously defined here and will have to wait for future work. By incorporating existing models of viscous interphase mechanics, we will be able to understand the effects of viscosity on fiber stress concentrations.

The database for fiber stress rupture is mainly limited to tests in air so dependence on oxygen concentration is lacking. SR competes with OE and IR at temperatures higher than about 1373 K for oxygen concentrations near 0.2%. The onset of SR occurs at 1373 K in air during dynamic crack growth according to our model and this onset is predicted to shift to 1423 K for lower oxygen concentrations. Without detailed data as a function of oxygen concentration, we cannot be more quantitative. The map suggests that SR shifts to higher temperatures as the oxygen concentration decreases. The boundary between FR and SR is suggested to occur at the fiber thermal limits. There is a need for additional stress rupture data as a function of oxygen concentration.

While thermal creep of polymer derived ceramic fibers is often non-linear, or viscous-like, in time and stress, irradiation creep of these same fibers appears to be linear in both time (dose) and applied stress. The fiber thermal creep has an activation energy of about 600 kJ/mol. The irradiation creep equation assumes a temperature independent regime below 1173 K (900 °C) and an activation energy of 50 kJ/mol for temperatures greater than 1173 K. The creep rate is linear in dose rate and stress. We observe that irradiation creep of the fibers dominates the fiber deformation process for temperatures below 1273 K (1000 °C) but thermal creep dominates at higher test temperatures, Fig. 4. This implies that we will need to further understand and model irradiation creep processes in SiC-based fibers since apparently that process is important in applications that operate at or below 1000 °C. There is little understanding of the mechanisms of irradiation creep in these fibers, whereas the thermal creep data can be understood by analogy to creep in viscous solids. The creep mechanisms in the fibers may be distinct from those that operate in the crystalline SiC-matrix just by virtue of the nanocrystalline nature of the fibers, even the stoichiometric fibers. The linear creep response suggests that a Nabarro-Herring creep mechanism may be operating but this remains to be shown conclusively.

4. Conclusion

A dynamic crack growth model with the following features has been developed: (1) it is based on the weight-function method using discrete fiber bridges, (2) it contains non-linear bridge extension laws based on fiber-creep kinetics for Nicalon-CG and Hi-Nicalon fibers, (3) it contains bridge extension laws for the case of interphase removal, and (4) it provides fully dynamic crack tracking using a critical-stress-intensity propagation criterion. The model reproduces the time-dependent crack growth kinetics observed experimentally in specimens of Nicalon-CG and Hi-Nicalon 0/90 woven composites. The transition from non-linear crack growth kinetics to linear growth kinetics is also reproduced by the model by comparing crack growth rates under FR or IR domination. Using the activation energy for the oxidation of carbon in the model it correctly predicted this change from non-linear to linear crack growth kinetics. By implementing a simple “fiber removal” algorithm, where the criterion for removal is based either on a critical oxide thickness or stress rupture threshold, we can also map out transitions between crack growth due to OE and SR. This model is being used to predict the effects of fiber stress rupture and neutron irradiation, where there is no data on composite material. A map of the crack growth mechanism as a function of environmental oxygen concentration and temperature was developed with assumption about the transition between mechanisms and this has been very effective in identifying optimum environmental regimes for using these materials. The model and resulting

mechanism map is helping us develop and understand crack growth mechanisms and to design improved composite materials.

Acknowledgements

This research was supported by Basic Energy Sciences, United States Department of Energy, under Contract no. DE-AC06-76RLO 1830 with Pacific Northwest National Laboratory, which is operated for the U.S. Department of Energy by Battelle Memorial Institute.

References

1. Henager Jr., C. H. and Jones, R. H., High-temperature plasticity effects in bridged cracks and subcritical crack growth in ceramic composites. *Mater. Sci. Eng., A*, 1993, **A166**, 211.
2. Henager Jr., C. H. and Jones, R. H., Subcritical crack growth in CVI silicon carbide reinforced with Nicalon fibers; experiment and model. *J. Am. Ceram. Soc.*, 1994, **77**, 2381.
3. Henager Jr., C. H., Jones, R. H., Windisch Jr., C. F., Stackpoole, M. M. and Bordia, R., Time dependent, environmentally assisted crack growth in Nicalon-fiber-reinforced SiC composites at elevated temperature. *Metall. Mater. Trans. A*, 1996, **27A**, 839.
4. Lewinsohn, C. A., Henager Jr., C. H. and Jones, R. H., Environmentally-induced failure mechanism mapping for continuous-fiber, ceramic composites. *Ceram. Trans.*, 1999, **96**, 351.
5. Bückner, H., *Z. Angew Math. Mech.*, 1970, **46**, 529.
6. Rice, J. R., Some remarks on elastic crack-tip stress fields. *Int. J. Solids Struct.*, 1972, **8**, 751.
7. Fett, T., Mattheck, C. and Munz, D., On the calculation of crack opening displacement from the stress intensity factor. *Eng. Fract. Mech.*, 1987, **27**, 697.
8. Marshall, D. B., Cox, B. N. and Evans, A. G., Mechanics of matrix cracking in brittle-matrix fiber composites. *Acta Metall.*, 1985, **33**, 2013.
9. Cox, B. N., Sridhar, N. and Argento, C. R., A bridging law for creeping fibers. *Acta Mater.*, 2000, **48**, 4137.
10. Cox, B. N. and Marshall, D. B., Stable and unstable solutions for bridged cracks in various specimens. *Acta Metall. Mater.*, 1991, **39**, 579.
11. Begley, M. R., Cox, B. N. and McMeeking, R. M., Time dependent crack growth in ceramic matrix composites with creeping fibers. *Acta Metall. Mater.*, 1995, **43**, 3927.
12. Begley, M. R., Evans, A. G. and McMeeking, R. M., Creep rupture in ceramic matrix composites with creeping fibers. *J. Mech. Phys. Sol.*, 1995, **43**, 727.
13. Begley, M. R., Cox, B. N. and McMeeking, R. M., Creep crack growth with small scale bridging in ceramic matrix composites. *Acta Metall. Mater.*, 1997, **45**, 2897.
14. Cox, B. N., Marshall, D. B., McMeeking, R. M. and Begley, M. R., Matrix cracking in ceramic matrix composites with fiber creep. *Solid Mech. Appl. Appl.*, 1997, **49**, 353.
15. Henager Jr., C. H. and Hoagland, R. G., Subcritical crack growth in CVI SiCf/SiC composites at elevated temperatures: Dynamic crack growth model. *Acta Materialia*, 2001, **49**, 3739.
16. DiCarlo, J. A., Required properties and test methods for high-temperature ceramic fiber reinforcements. *Ceramurgia*, 1998, **28**, 88.
17. Windisch Jr., C. F., Henager Jr., C. H., Springer, G. D. and Jones, R. H., Oxidation of the carbon interface in Nicalon-fiber-reinforced silicon carbide composite. *J. Am. Ceram. Soc.*, 1997, **80**, 569.
18. Zhu, Y. T., Taylor, S. T., Stout, M. G., Butt, D. P. and Lowe, T. C., Kinetics of thermal, passive oxidation of Nicalon fibers. *J. Am. Ceram. Soc.*, 1998, **81**, 655.
19. DiCarlo, J. A., Yun, H. M., Morscher, G. N. and Goldsby, J. C., Models for the thermostructural properties of SiC fibers, in high-temperature ceramic-matrix composites II. *Ceram. Trans.*, 1995, **58**, 343.
20. Glime, W. H. and Cawley, J. D., Stress concentration due to fiber–matrix fusion in ceramic-matrix composites. *J. Am. Ceram. Soc.*, 1998, **81**, 2597.
21. Nair, S. V., Jakus, K. and Lardner, T. J., Mechanics of matrix cracking in fiber reinforced ceramic composites containing a viscous interface. *Mech. Mater.*, 1991, **12**, 229.
22. Yun, H. M. and DiCarlo, J. A., Time/temperature dependent tensile strength of SiC and Al2O3-based fibers. *Ceram. Trans.*, 1996, **74**, 17.
23. Tressler, R. E. and DiCarlo, J. A., Creep and rupture of advanced ceramic fiber reinforcements, in high-temperature ceramic-matrix composites I. *Ceram. Trans.*, 1995, **57**, 141.
24. Price, R. J., Properties of silicon carbide for nuclear fuel particle coatings. *Nucl. Technol.*, 1977, **35**, 320.
25. Scholz, R., Mueller, R. and Lesueur, D., Light ion irradiation creep of Textron SCS-6 silicon carbide fibers. *J. Nucl. Mater.*, 2002, **307–311**, 1183.
26. Abbe, F., Vicens, J. and Chermant, J. L., Creep behavior and microstructural characterization of a ceramic matrix composite. *J. Mater. Sci. Lett.*, 1989, **8**, 1026.
27. Chermant, J. L., Abbe, F. and Kervadec, D., On the creep of long ceramic fibers reinforced ceramic matrix. In *Creep Fract. Eng. Mater. Struct., Proc. Int. Conf. 5th*, 1993, p. 371.
28. Wu, X. and Holmes, J. W., Tensile creep and creep-strain recovery behavior of silicon carbide fiber/calcium aluminosilicate matrix ceramic composites. *J. Am. Ceram. Soc.*, 1993, **76**, 2695.
29. Grathwohl, G., Meier, B. and Wang, P., Creep of fiber and whisker reinforced ceramics, glass-ceramics and glasses. *Key Eng. Mater.*, 1995, **108–110**, 243.
30. Evans, A. G. and Weber, C., Creep damage in SiC/SiC composites. *Mater. Sci. Eng., A*, 1996, **A208**, 1.
31. Mumm, D. R., Morris, W., Dadkhah, M. S. and Cox, B. N., Subcritical crack growth in ceramic composites at high temperature measured using digital image correlation, in thermal and mechanical test methods and behavior of continuous-fiber ceramic composites. *ASTM Spec. Tech. Publ.*, 1997, **STP 1309**, 102.
32. Mizuno, M., Zhu, S., Kagawa, Y. and Kaya, H., Stress, strain, and elastic modulus behavior of SiC-fiber/SiC composites during creep and cyclic fatigue tests. *Key Eng. Mater.*, 1997, **132–136**, 1942.
33. Cox, B. and Zok, F., Recent advances in fibrous ceramic composites. In *Brittle Matrix Compos. 5, Proc. Int. Symp., 5th*, 1997, p. 497.
34. Wilshire, B., Carreno, F. and Percival, M. J. L., Tensile creep and creep fracture of a fiber-reinforced SiC/SiC composite. *Scr. Mater.*, 1998, **39**, 729.
35. Chermant, J.-L. and Boitier, G., The importance of damage and slow crack growth in the creep behavior of ceramic matrix composites. *Adv. Compos. Mater.*, 1999, **8**, 77.
36. Zhu, S., Mizuno, M., Kagawa, Y., Cao, J., Nagano, Y. and Kaya, H., Creep and fatigue behavior in Hi-Nicalon-fiber-reinforced silicon carbide composites at high temperatures. *J. Am. Ceram. Soc.*, 1999, **82**, 117.
37. Tressler, R. E., Rugg, K. L., Bakis, C. E. and Lamon, J., Effects of matrix cracking on the creep of SiC–SiC microcomposites. *Key Eng. Mater.*, 1999, **164/165**, 297.
38. Evans, A. G., Zok, F. W., McMeeking, R. M. and Du, Z. Z., Models of high-temperature, environmentally assisted embrittlement in ceramic-matrix composites. *J. Am. Ceram. Soc.*, 1996, **79**, 2345.
39. Heredia, F. E., McNulty, J. C., Zok, F. W. and Evans, A. G., Oxidation embrittlement probe for ceramic matrix composites. *J. Am. Ceram. Soc.*, 1995, **78**, 2097.